Dissociation of thixotropic clay gels

Céline Martin,[1] Frédéric Pignon,[1] Jean-Michel Piau,[1] Albert Magnin,[1,*] Peter Lindner,[2] and Bernard Cabane[3]
[1]*Laboratoire de Rhéologie, Université Joseph Fourier, Grenoble I, Institut National Polytechnique de Grenoble, CNRS UMR 5520, Boîte Postale 53, 38041 Grenoble Cedex 9, France*
[2]*Institut Laue-Langevin, Boîte Postale 156, F-38042 Grenoble Cedex 9, France*
[3]*Laboratoire PMMH, ESPCI, 10 Rue Vauquelin, 75231 Paris Cedex 5, France*
(Received 22 December 2000; revised manuscript received 14 February 2002; published 12 August 2002)

Laponite dispersions in water, at moderate ionic strength and high *p*H, are thixotropic: depending on previous history, they can be fluids or gels. The mechanisms of the fluid-gel and gel-fluid transitions have been examined through ionic analysis of the aqueous phase, static light, and small-angle neutron scattering, rheological experiments, and centrifugation. The results indicate that the particles attract each other in edge-to-face configurations. These attractions cause the particles to gather in microdomains, which subsequently associate to form very large fractal superaggregates, containing all the particles in the dispersion. A gel state is obtained when the network of connections is macroscopic. This network is destroyed by the application of sufficient strain, but it heals at rest. The addition of peptizers weakens the edge-to-face attractions, and makes the healing times much slower.

DOI: 10.1103/PhysRevE.66.021401 PACS number(s): 82.70.Kj, 83.80.Hj

I. INTRODUCTION

This study focuses on the nature of interactions between nanometric clay particles in aqueous dispersions. The material used for this work was an aqueous dispersion of laponite, which is a synthetic clay of the hectorite type [1]. This clay consists of particles that are shaped as thin disks (or platelets), with an average diameter of 30 nm, and an average thickness of 1 nm [1,2].

In aqueous dispersions, the particles are ionized, with a large number of negative charges along the faces of the platelets, and a few positive charges along the edges [1]. These surface charges are compensated by Na^+ counterions, which are distributed next to the negative surface charges and also in a diffuse layer surrounding each particle. The main interactions between particles are electrostatic interactions between these anisotropic charge distributions. In addition there are also weak van der Waals attractions and excluded volume repulsions.

The aqueous dispersions of laponite particles have unusual properties. At moderate volume fractions ($0.5\% < \phi_\nu < 3\%$), they form gels that are capable of suspending large solid particles. These gels are easily broken by applied forces. When large continuous deformations are applied, they give way to a fluid state. Upon cessation of flow, this fluid state is retained for a while. Finally, the material heals slowly and becomes a gel again. This behavior is called thixotropy. It is the basic reason for the use of laponite in many practical applications [1].

The mechanism of gel formation and the nature of processes that cause thixotropy in clay dispersions have been much debated [2–30]. In particle dispersions, there are two general mechanisms that may cause gel formation. The first one originates from interparticle attractions or adhesion. In this case, the particles aggregate to form a connected network that extends throughout the material. This mechanism is most commonly found in protein gels [31] and also in gels made of aggregated mineral particles [32,33]. The second one originates from interparticle repulsions. In this case, solidlike behavior originates from the lack of free volume: each particle becomes unable to move because every location around it is already occupied by another particle [27–29,34,35].

In laponite dispersions, evidences for both mechanisms have been found, but in different regions of the phase diagram [15–17,25–29].

At very low ionic strengths (10^{-4} mol l^{-1} and below), the electrostatic interactions are very long-range type. Indeed, the Debye length, κ^{-1}, is comparable to the particle diameter. In these conditions, the anisotropy of the charge distribution around each particle becomes unimportant. The particles interact through overlap of their ionic diffuse layers, which yields repulsions with a range κ^{-1}. When the volume fraction of particles is sufficiently low, the ionic layers do not overlap, and the particles can move (fluid state). When this volume fraction is high enough, the ionic layers are forced to overlap, and the particles become unable to move (gel state) [27–29]. The critical volume fraction that separates the fluid from the gel can be evaluated as [36]

$$\phi_\nu^* = 0.64 \frac{3}{2} \frac{H}{2R} \frac{1}{(H/2R + \kappa^{-1}/R)^3} = 0.48 \frac{HR^2}{(H/2 + \kappa^{-1})^3},$$

where R is the particle radius and H its thickness. Typically, for a sodium ion concentration of 10^{-4} mol l^{-1}, the Debye length κ^{-1} is 30 nm, and the critical volume fraction is $\phi_\nu^* = 0.4\%$.

In this regime, when the ionic strength is raised, the ionic screening becomes more efficient, the Debye length κ^{-1} is shorter, and the critical volume fraction ϕ_ν^* is higher. This is indeed observed in laponite dispersions at very low ionic strengths: in the phase diagram, the fluid-to-gel boundary shifts to higher volume fractions when the ionic strength is

*Corresponding author. Email address: Magnin@ujf-grenoble.fr

raised from 10^{-5} to 10^{-4} mol l^{-1} [28]. This shift is typical of gels formed by interparticle repulsions; indeed, the higher ionic strength reduces these repulsions and makes free volume available for particle motions. Other experiments confirm that, in this regime, gel formation is caused exclusively by repulsions between particles: in particular, light scattering experiments demonstrate that the gel can be completely homogeneous, and therefore free of any aggregation process [27,29]. In this regime, the colloidal gel has also been called a colloidal glass, because motions are inhibited through lack of free volume, as in glass [27,29].

At moderate ionic strengths (10^{-3} mol l^{-1} and above), the electrostatic interactions are of short range. In these conditions, the anisotropy of the charge distribution around each particle controls their interactions. These interactions may be repulsive in some configurations of the particles (e.g., in the parallel ''stacked plates'' configuration), and attractive in others (e.g., in the ''house-of-cards'' structure). At these ionic strengths, it is found that the particles tend to aggregate spontaneously, forming microdomains that have a higher particle density than the surrounding medium and sizes on the order of 1 μm [21]. At very long times, these microdomains become interconnected and build a fractal aggregate structure, up to length scales of many micrometers. Simultaneously, the dispersion becomes a gel, with mechanical properties that depend on the fractal dimension of the aggregates. Concentrated dispersions become gels relatively fast, dilute dispersions much slower or not at all. Accordingly, a fluid-to-gel boundary has been determined. In the phase diagram, this boundary shifts to lower volume fractions when the ionic strength is increased [15], which is a further indication that gel formation results from an aggregation process. Indeed, the higher ionic strength reduces repulsions that would otherwise prevent aggregation of particles. A variation of this salt induced aggregation is the aggregation promoted by the release of Mg^{2+} ions, which may occur in dispersions equilibrated at low pH [26].

Still, the precise mechanism of this aggregation is not known: the debate about the aggregate structure, i.e., house of cards or stacked plates, has been going on for decades. Moreover, a central question for the applications of laponite is how the aggregation process may or may not cause the thixotropy of the gels, i.e., their ability to become fluids upon continuous deformation, and to heal back to the gel state when left to rest.

Here we examine gel formation and dissociation in the regime of moderate ionic strength, aiming at a more precise determination of interactions between particles. For this purpose, we modify the surface charges around the clay particles by adding peptizers. Then, we compare the original laponite dispersions with a dispersion containing peptizers. These peptizers are salts in which the anions can bind to positive surface charges on edges of platelet shaped particles. In this way they reduce the edge-to-face attractions, by making the edges less positively or even negatively charged. This should reduce the occurrence of edge-to-face links between particles. Moreover, these added salts also increase the general electrostatic screening. They have the same effects as simple salts, i.e., increasing free volume but also making nonspecific associations easier. Thus, the addition of peptizers in laponite dispersions could change the nature of interactions between clay particles, going from specific edge-to-face attractions to nonspecific repulsions or attractions.

In a first step, we examine the effect of peptizers on ionic compositions of the aqueous phase that disperses the particles. The modifications of ionic content during swelling and aging of the dispersions are evaluated. Next, the structure of the dispersions, i.e., the spatial distributions of particles, is determined through small-angle neutron and static light scattering. Then rheometric measurements are performed in shear deformations. They characterize the transient response of the dispersions to an applied shear rate, their yield stress and their stress level maintained during steady shear flow and the recovery of the gel structure after destructuration by shear flow. Finally, the connectivity of the dispersions is examined through centrifugation experiments that cause the aggregates to separate from the aqueous phase.

The results are also used to make a model for the network of interparticle links, and for the changes that are brought by peptizers to this network. In this way, a qualitative interpretation for the thixotropy of laponite dispersions can be proposed.

II. MATERIALS AND METHODS

A. Materials

In this study we used the synthetic clay, laponite XLG, manufactured by Laporte Industries. Its chemical composition is 66.2% SiO_2, 30.2% MgO, 2.9% Na_2O, and 0.7% Li_2O, corresponding to the following chemical formula [10]:

$$Si_8[Mg_{5.45}Li_{0.4}H_4O_{24}]^{0.7-}Na_{0.7}^{0.7+}.$$

This clay is made of small platelet or disk-shaped particles with an average diameter $2R=30$ nm and a thickness $H=1$ nm [1,2]. The density of the particle is $\rho_p = 2.53$ g cm^{-3} [4]. Each particle has a central layer made of Mg^{2+} cations in octahedral coordination to oxygen atoms or hydroxyl groups; this central layer is sandwiched between two silicate layers where the silica atoms are in tetrahedral coordination to oxygen atoms [1]. The total thickness of these three layers is about 1 nm [1]. Some of the Mg^{2+} sites of the central layer are substituted with Li^+ cations. This creates a charge inbalance, which is compensated by Na^+ counterions located at the surface of the outer layers.

In water, these Na^+ counterions are hydrated and released in a diffuse layer surrounding the particle. Consequently, the platelet carries a negative surface charge, which amounts to about 700 charges per particle, or a surface charge density of 0.7 electron nm^{-2} on each face. The edges of the platelets, however, carry some Mg-OH sites which are weak bases; at pH<11, some of these groups bind protons and then become positively charged Mg-OH_2^+ sites. According to the manufacturer, the number of these charges is on the order of 60 charges per particle, which gives a linear charge density of 1.4 charge nm^{-1} [1]. Finally, at high pH, some of the surface sites may become ionized as SiO^- groups.

The result of all these ionization processes is that the faces of the platelets carry a strong negative charge, while the edges carry a positive charge, thereby making an edge-to-face interaction favorable [37].

Peptizers are commonly used to control these edge-to-face interactions [1]. The peptizer used here was tetrasodium diphosphate (abbreviated to tspp hereafter), obtained from Prolabo. Its chemical formula is $Na_4P_2O_7$, $10H_2O$ and its molecular mass is 446 g mol^{-1}. In water, it releases $P_2O_7{}^{4-}$ groups which bind to the Mg-$OH_2{}^{+}$ sites on the edges of the platelets. Consequently, the aggregation of the particles is delayed, and the dispersion remains fluid for a longer time interval after preparation. Peptizer concentrations C_p are given as percentages of the mass of dry clay.

The dispersions were prepared in two ways, depending on the final clay concentration. For the more concentrated dispersions, the peptizer was dispersed in a solution of double-distilled water and sodium chloride with an initial ionic strength of 10^{-3} mol l^{-1}, using ultrasounds at a frequency of 20 kHz and a power level of 350 W for a period of 10 s. The dry clay was then added and mixed using ultrasounds at a frequency of 20 kHz and power level of 350 W for a period of 10 min. The volume fractions obtained by this method were $\phi_v = 3.3\%$ with $C_p = 0\%$, and $\phi_v = 6-8\%$ with $C_p = 6\%$. For the less concentrated dispersions, the peptizer and the dry clay were stirred with a mixer in the same initial solution during, respectively, 5 min and 30 min.

Laponite dispersions were stored in large quantities (1 kg) in tightly closed jars, in order to minimize exposure to ambient air. Thus, the *p*H evolution was governed by clay dissolution only during the swelling of the clay. As a result, the *p*H increased and stabilized to an equilibrium value near *p*H 10.

Changes were observed in the viscoelastic properties and structural characteristics of the gels over time. This is due, in part, to the osmotic swelling caused by repulsion between the double layers and also to the progressive organization of the particles into fractal aggregates over larger length scales [21]. In order to take into account these structural and mechanical changes in the dispersions, the time t_p that elapsed between the end of preparation and the test will always be indicated in the remainder of this text.

B. Ionic analysis

The composition of the aqueous phase that dispersed the particles was analyzed in the following way. Dispersions were centrifuged at an acceleration of 50 000 g_a (with $g_a = 9.81$ m s^{-2}) for at least 14 h. This time corresponds to permanent conditions where all the particles have settled. The supernatants were recovered and used for the analysis of sodium and magnesium ions. The measurements were performed at the ESIGEC laboratory in Chambéry, using an atomic absorption spectrometer. This consists of an appropriate burner for an acetylene/air flame and a hollow cathode lamp with a wavelength $\lambda = 589$ nm. For the sodium analysis, the supernatants were diluted, in conformity with current standards, with a solution of nitric acid, thus reducing the *p*H to about 2. For the magnesium analysis, they were diluted with a solution of lanthanum chloride and chlorhydric acid.

The conductivity and *p*H of the supernatants were also measured with classical instruments at a temperature of 25 °C.

C. Scattering techniques

The structure of the dispersions was examined through static light scattering (SLS) and small-angle neutron scattering (SANS). These experiments measure a scattered intensity I as a function of a scattering vector Q. For isotropic samples, only the magnitude Q of the scattering vector is relevant, and is determined by the wavelength of the incident radiation, λ, the refractive index of the scattering medium, n, and the scattering angle, θ, according to

$$Q = \left(\frac{4\pi n}{\lambda}\right)\sin\left(\frac{\theta}{2}\right).$$

The SLS measurements covered a range of scattering vectors extending from 4×10^{-5} to 5×10^{-4} Å^{-1} and the SANS measurements covered an additional range extending from 10^{-3} to 10^{-1} Å^{-1}. Thus, this combination made it possible to obtain structural information ranging from the size of a particle (a few nanometers) to that of the largest structures (a few micrometers).

The small-angle neutron scattering measurements were carried out at the Institut Laue-Langevin in Grenoble, using the D11 multidetector [38], at a wavelength of 6 Å. The distances between the detector and the sample were fixed at 2.5, 10, and 35.7 m with beam collimations of 2.5, 10, and 40.5 m, respectively. The measurements were performed in 1-mm-thick Suprasil quartz cells. The radial mean of the total scattering intensity was then calculated using classical integration software.

The laser bench developed and built at the Laboratoire de Rhéologie [39–41] was used for the static light scattering measurements. It consists of a 2-mW laser beam (He-Ne) with a wavelength of 6328 Å, and a Fresnel lens (focal distance 122 mm and diameter 127 mm) acting as a scattering screen. A beam stop cuts off beam transmission. The detector is a video camera with a 752×582 pixel charge coupled device sensor. A shutter was used to vary the acquisition time from $\frac{1}{50}$ to $\frac{1}{10\,000}$ s. The results were analyzed by means of image processing and a program for carrying out classical integration operations.

The samples were placed between two glass slides in a parallel-sided cell. They had a constant thickness of 0.3 mm, such that the transmission measurements gave satisfactory results ($I_{\text{transmitted}}/I_{\text{incident}} = 0.95$) regardless of the volume fraction. Two kinds of measurements were performed. First, the structure at rest was determined for both dispersions. The samples were left to rest in the cell for 10 min., as they may have suffered mechanical stresses and partial loss of structure during the placement between the slides. Successive measurements were performed at different times after the samples had been installed to check that this period was sufficiently long for the results not to be affected by any pos-

sible structural reorganization. Then, the changes occurring as the dispersions recover their structure, after applying a constant shear rate, were monitored.

D. Rheometric techniques

The rheometric behavior of the laponite dispersions under shear was studied using a Weissenberg-Carrimed-type controlled speed rotating rheometer. The tests were carried out at a temperature of (22 ± 1) °C. Several rheometric procedures were used.

Start-up shearing tests were performed with cone-plate configurations of various dimensions. The tools, made of steel or plexiglas, were covered with glass paper of 200 μm roughness, except around the central part of the cone, so as to reduce interface effects and particularly slip phenomena. Torsion bar torque sensors were used. The atmosphere around the sample was saturated with water to avoid evaporation during the measurement [42]. In these start-up tests, a constant shear rate was suddenly applied to the sample whose initial state is controlled. The transient response under stress was recorded until steady conditions were achieved. The stress levels for the steady regime were then used to establish flow curves for the dispersions under shear.

Dynamic tests described in earlier works [18,21] were also performed to evaluate the response of thixotropic gels. The structure of the sample was destroyed by preliminary shearing at a constant rate of 50 s^{-1} during 5 min. Shearing was stopped and structural recovery was monitored by measuring the change in elastic modulus G' and viscous modulus G'' at a fixed frequency of 0.1 Hz and strain of 5%. The frequency and strain were chosen in such a way that the material remained within the linear viscoelastic domain and the measurement time was short in comparison with the time taken for the material to recover its structure [21].

E. Centrifugation

The effect of centrifugation on laponite dispersions was studied using a Heræus centrifuge with a range of accelerations extending up to $50\,377g_a$. The tests were run at a temperature of 20 °C for an acceleration of $50\,000g_a$, at which the liquid and solid phase, referred to, respectively, as the supernatant and deposit, were separated. An initial state was given to the dispersions during the filling of the centrifugation tubes. Using a syringe with a shear rate of about 50 s^{-1} induced the destructuration of the dispersions. Centrifugation runs were started instantaneously after the filling of the tubes.

Several procedures were used to characterize the dispersions of laponite under compression. The depth of the deposits was plotted as a function of time, in order to determine the mechanical strength of these dispersions. The mass of dry matter was weighed, precisely to within 0.1 mg, by drying the supernatants at a temperature of 120 °C. The mean particle mass and volume fractions of, respectively, the supernatant and the deposit could thus be deduced.

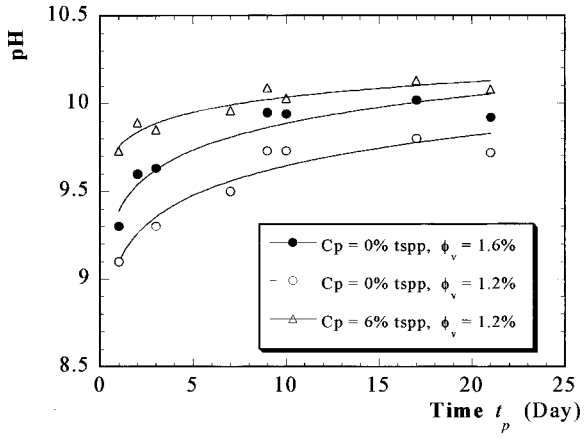

FIG. 1. pH versus age of laponite dispersions at different volume fractions and peptizer concentrations.

III. RESULTS

A. Ionic composition of the aqueous phase

The interactions of particles in the laponite dispersions are influenced by the ionic composition of the aqueous phase: monovalent cations can screen the repulsions due to overlap of ionic layers, and they are known to cause fast flocculation when their concentration exceeds 10^{-2} mol l^{-1} [15]. Also, divalent cations can cause even more efficient screening and bridge particles together, leading to gel formation or flocculation [26]. Therefore, it is extremely important to know accurately the ionic composition of the aqueous phase that disperses the particles.

The composition of this aqueous phase is determined by (i) dissociation of added salts, (ii) dissolution of the laponite particles, and (iii) absorption and ionization of CO_2 from ambient air. The dissolution of laponite is known to be significant at neutral to low pH, and it may be accelerated if carbonic acid makes the dispersions acidic. As explained above, precautions were taken to minimize exposure to ambient air, but this possibility was checked anyway. This dissolution proceeds through the following reaction [10]:

$$Si_8Mg_{5.45}Li_{0.4}H_4Na_{0.7}+12H^+ + 8H_2O \rightarrow 0.7Na^+ + 8Si(OH)_4 + 5.45Mg^{2+} + 0.4Li^+.$$

Accordingly, the availability of H^+ ions would cause the release of magnesium and sodium ions. Conversely, the dissolution of laponite in a closed vessel will use H^+ ions and therefore cause the pH to rise until the dissolution stops for lack of H^+. In our experiments, large amounts of laponite dispersions were kept in closed jars. The pH was then found to rise to about 10, as expected for a closed vessel (Fig. 1).

The concentration of H^+ ions that were available from the distilled water at pH 5 used for the preparation is 10^{-5} mol l^{-1}. According to the reaction scheme, the concentration of released ions is 4.5×10^{-6} mol l^{-1} for Mg^{2+} ions and 6×10^{-7} mol l^{-1} for Na^+ ions. These amounts of released ions are quite small. They can be compared with the total amounts of these ions in solution, which may originate from other sources (e.g., added salts).

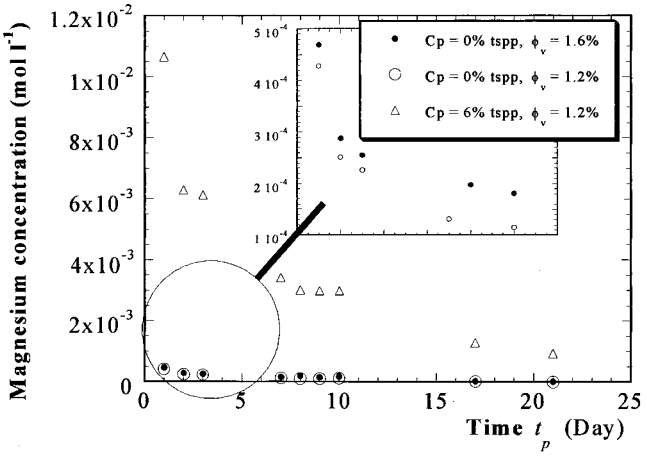

FIG. 2. Magnesium ions concentration versus age of laponite dispersions at different volume fractions and peptizer concentrations.

The measured concentrations of magnesium ions (Fig. 2) show a steady decrease with time, which may be caused by the precipitation of $Mg(OH)_2$ at high pH. In dispersions with no added peptizer, the initial concentration of Mg^{2+} ions was 4.5×10^{-4} mol l^{-1} and it decayed to 10^{-4} mol l^{-1} in 20 days. This behavior is opposite to that observed by Mourchid and Levitz [26] for samples kept in contact with ambient atmosphere, where the Mg^{2+} concentration started at the same level but then rose to 10^{-3} mol l^{-1} over a year, as the samples became gels. Therefore the behavior of dispersions that are kept in closed jars is not caused by the release of Mg^{2+} ions: there is, initially, a small amount of such ions that originate from salts produced by the synthesis, and these ions are progressively eliminated through precipitation. For dispersions with added peptizers, the concentrations of Mg^{2+} ions are much higher, starting at 10^{-2} mol l^{-1} and decaying to 10^{-3} mol l^{-1} in 20 days. These higher concentrations obviously result from complexation of magnesium ions by the peptizers. Again, these ions play no role in the gel formation process.

The concentrations of sodium have been measured and show no substantial change during the aging of the dispersions. They are equal to 6.5×10^{-3} mol l^{-1} in dispersions without peptizer, and 2×10^{-2} mol l^{-1} in dispersions that contain 6% of peptizers. These ions must originate from salts that were produced by the synthesis, or from the peptizers. These concentrations are enough to produce substantial screening of interparticle repulsions: the corresponding Debye lengths are 4 nm for dispersions without peptizers and 2 nm with peptizers, i.e., much less than the average interparticle distance.

According to the phase diagram established by Mourchid *et al.* [15], concentrated dispersions without any peptizer are in a gel state when the ionic strength is below 10^{-2} mol l^{-1}, and in a flocculated state when it is above this limit. However, our dispersions with added peptizers have an ionic strength that is much in excess of this limit. Yet these dispersions are either homogeneous fluids or transparent gels, with no sign of phase separation. The peptizer, therefore, prevents moderately concentrated systems from flocculating.

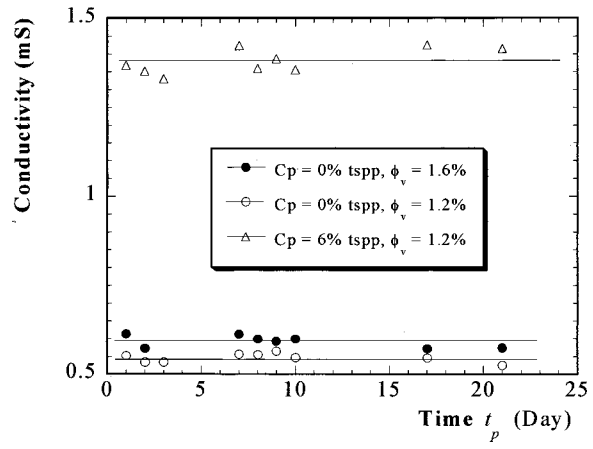

FIG. 3. Conductivity versus age of laponite dispersions at different volume fractions and peptizer concentrations.

The evolution of the total ionic concentrations was also monitored through conductivity measurements (Fig. 3). The results show very little evolution over a period of 20 days, thereby confirming that no substantial dissolution takes place in the conditions of our experiments.

In conclusion, the dissolution of laponite particles in water at high pH releases few ions. Changes in ionic concentrations are thus too small to cause a substantial change in the interactions of particles, and cannot be the cause of observed sol-gel transitions.

B. Structure according to scattering experiments

A general view of the modifications in structure produced by the addition of peptizers can be seen in the scattering curves shown in Fig. 4. These scattering curves have been obtained by combining small-angle neutron and static light scattering data so that the magnitudes of the slope of the two sets of data matched each other in a log-log graph. The wave vector domain covered by the data extends from interparticle dimensions $Q=10^{-1}$ Å^{-1} to the largest organized structures

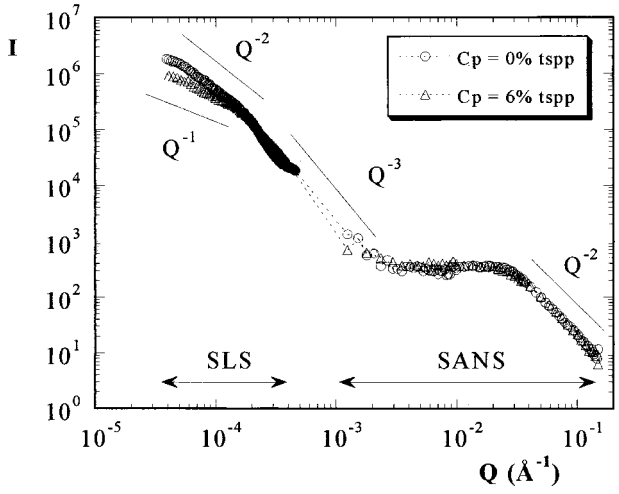

FIG. 4. Small-angle neutron scattering and static light scattering of laponite dispersions at rest made using different peptizer concentrations. $\phi_v=3.33\%$ and $t_p=15$ days.

$Q=4\times10^{-5}$ Å^{-1}. The curves of dispersions without peptizer are from our previous work [21]; the curves of dispersions with peptizers are additional ones. They show remarkable features: the peptizer has no effect on the interparticle and intraparticle organization at the small scales observed by small-angle neutron scattering, but it does change the organization at the large scales observed by static light scattering.

1. Structure at small length scales

We examine here the right part of the Fig. 4 where the wave vector Q is larger than 10^{-3} Å^{-1}, for laponite dispersions at volume fraction of 3.33%.

At high wave vector values ($Q>3\times10^{-2}$ Å^{-1}), it appears that, for both dispersions, the scattering intensity by SANS at small length scales follows a Q^{-2} power law. This decay is characteristic of the scattering intensity of discotic particles with no preferential orientation.

Then, at Q values corresponding to distances between neighboring particles ($Q=3\times10^{-2}$ to 3×10^{-3} Å^{-1}, $d=21-210$ nm), the scattering curves show a plateau. This plateau is due to interparticle interferences. Accordingly, density fluctuations must be suppressed in this domain of wave vectors, i.e., the number density of particles is uniform over the corresponding scales. Note that no scattering peak is observed at the interparticle distance. This is typical of repulsive correlations between anisotropic objects that have no orientational correlations. Interestingly, the addition of peptizers has absolutely no effect on the scattering curves in this range of Q. Consequently, the correlations of positions and orientations of neighboring particles are the same, regardless of whether or not peptizers have been added.

Finally, at smaller wave vector values ($Q<3\times10^{-3}$ Å^{-1}, $d>210$ nm), the scattered intensity is higher than the intensity of the plateau. This scattering excess originates from fluctuations in the number density of particles, i.e., the alternation of dense areas (microdomains) and less dense ones (voids) [21].

2. Large-scale aggregation

The organization of the dispersions at still larger scales is reflected in the light scattering data. We examine here the left part of the Fig. 4 where the wave vector Q is smaller than 5×10^{-4} Å^{-1}, for laponite dispersions at volume fraction of 3.33%.

The high wave vector part of the light scattering curves is a continuation of the Q^{-3} power law already observed in the small-angle neutron scattering results. This scattering is produced by the alternation of dense microdomains and voids, as mentioned above, and the Q^{-3} power law indicates that these microdomains do not have an odd shape, e.g., they are neither anisotropic nor fractal. The largest size of these microdomains is indicated by the lowest boundary of the Q^{-3} power law; it is 3–4 μm for dispersions with and without peptizers, respectively.

At the lowest wave vector values ($Q<2\times10^{-4}$ Å^{-1}), the structural organization becomes a mass fractal (Figs. 4 and 5). The fractal dimension (noted D_f in the following) of these superaggregates is given by the slope of the scattering

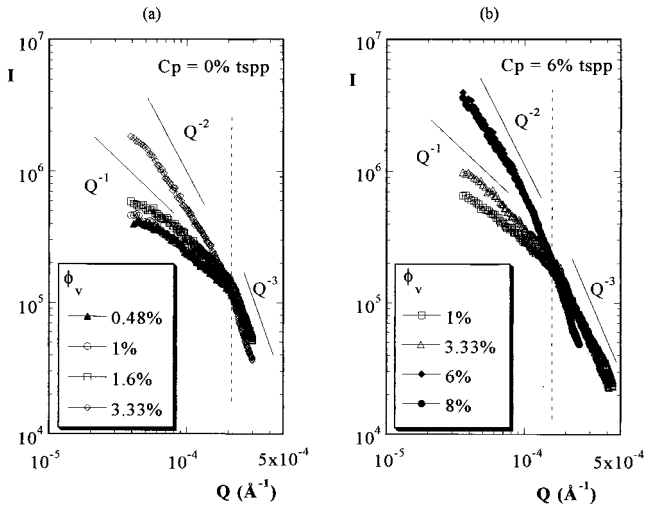

FIG. 5. Static light scattering of laponite dispersions at rest made using different peptizer concentrations and different volume fractions. $t_p=15$ days. (a) $C_p=0\%$ tspp, (b) $C_p=6\%$ tspp.

curves. The exponent of the power law changes with the addition of peptizers. In the case of dispersions that contain peptizers, the slope is close to Q^{-1}, corresponding to a linear organization. In the case of dispersions that contain no peptizer, the slope is close to Q^{-2}, corresponding to a denser aggregation of the microdomains. Furthermore, Fig. 5 shows the effect of the clay volume fractions on the slope of the scattering intensity, in this domain of wave vectors. All these scattering curves have been obtained at identical aging times after the preparation of the dispersions. For this set aging time, it appears that the power law changes from a very weak slope to a steeper slope, with higher volume fractions for both dispersions with and without peptizers. This reflects a higher rate of aggregation of the microdomains when the overall volume fraction is higher.

Accordingly, the large-scale structure of the dispersions is made by the aggregation of microdomains into superaggregates that have a fractal structure. The rate of this aggregation is considerably reduced by the addition of peptizers.

C. Mechanical properties under flow

The addition of peptizers to laponite dispersions has spectacular effects on their mechanical behavior. At the volume fractions used here (1.2% and 1.6%), dispersions with no peptizer added behave as physical gels, whereas dispersions with peptizers behave as viscous fluids. This overall appreciation needs to be qualified in order to define in which ways these dispersions behave as gels or fluids. For this purpose, several types of experiments have been performed: (i) measurements of the resistance to steady shear flow, (ii) evaluation of the thixotropic behavior by measurements of the transient response to constant shear rate, and (iii) measurements of the resistance to small amplitude deformations while the system is relaxing after the cessation of shear flow.

1. Steady shear flow properties

Laponite dispersions can be forced to flow by the application of sufficient strain. Their stress levels in steady shear

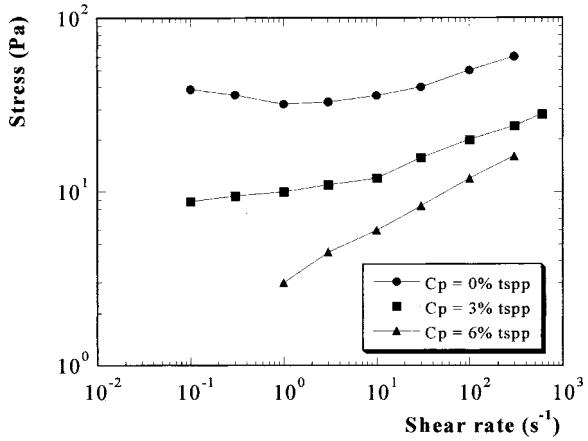

FIG. 6. Steady flow curve of laponite dispersions at different peptizer concentrations at a temperature of 22 ± 1 °C. $\phi_v=1.2\%$ and $t_p=25$ days.

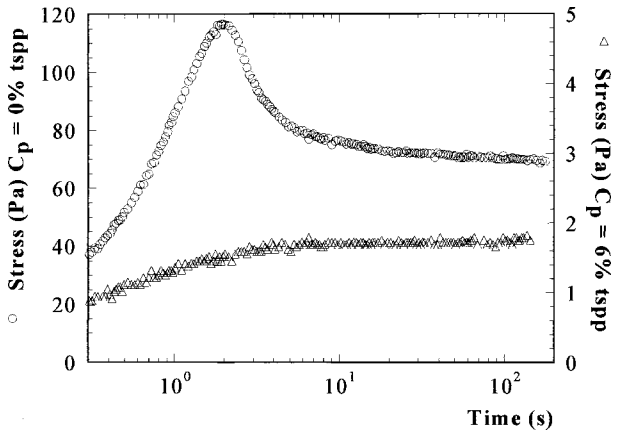

FIG. 7. Transient response of laponite dispersions at shear rate of 0.1 s^{-1} after shearing at 50 s^{-1} during 5 min followed by a rest period of 5 min, at a temperature of 22 ± 1 °C. $\phi_v=1.6\%$ and $t_p=53$ days.

flow are represented in Fig. 6. These curves show the influence of peptizers on the shear stresses of the dispersions when a constant shear rate is applied.

It appears that dispersions that contain no peptizer follow stress curves with a minimum. These results have already been analyzed by Pignon, Piau, and Magnin [18]. The stress levels at very low shear rates tend toward a yield stress value corresponding to the dynamic yield stress of the gelled dispersions. The stress plateau is associated with a particular mode of deformation, in which all shear is localized in a thin layer of the sample. At high shear rates, the stress increases and shear is homogeneous throughout the bulk of the sample.

In contrast, the dispersions containing peptizers flow more easily, especially so at lower shear rates where the stress levels are reduced by more than one order of magnitude. The dynamic yield stress is reduced (at intermediate peptizer concentrations) or nonexistent (at the highest concentration). In that case the gel-like behavior has completely vanished.

These results indicate that the network of mechanical links that produces the solidlike behavior of pure laponite dispersions has been weakened or dissociated by the addition of peptizers. At this stage, the nature of these connections is not known: they may be chemical links between particle surfaces, or physical forces with no direct contact between particles.

2. Thixotropy

The thixotropic behavior of laponite dispersions is illustrated by two kinds of results: destruction of the network by shear, and recovery after the cessation of shear. Figure 7 represents the transient response of dispersions when a constant shear rate of 0.1 s^{-1} is applied. In order to have a controlled initial state of the dispersions, a shear rate of 50 s^{-1} has been previously applied during 5 min and the dispersions have been let to rest during 5 min.

Dispersions that contain no peptizer follow a curve characteristic of gelled dispersions. At short times, stress increases linearly with time: the sample deformation is elastic. Then, stress is maximal and is related to the yield stress of the dispersion. Beyond this maximum, the dispersion begins to flow and the stresses are relaxed until a steady regime. This decrease corresponds to breakdown of the network [24].

For dispersions that contain peptizers, the transient response is different and characteristic of viscoelastic dispersions. The maximum in stress disappears by adding peptizers. However, at short times, the deformation of the dispersions produces a weak elastic response and at long times, the steady regime is also established.

Figure 8 presents the recovery of the mechanical response in dispersions that were sheared at 50 s^{-1} during 5 min, and abruptly brought to rest. In dispersions that contain no peptizer [Fig. 8(a)], the cessation of flow is followed almost instantly by recovery to a state where the elastic modulus G' is superior to the viscous modulus G''. This mechanical response is representative of a solidlike behavior. Then both moduli evolve according to two characteristic times. Initially,

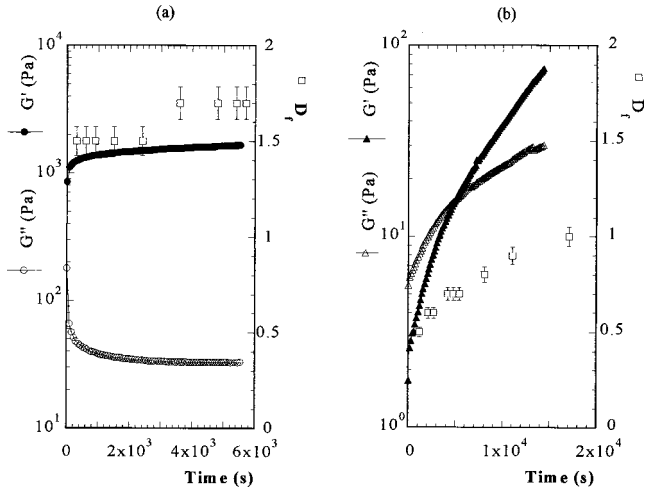

FIG. 8. Dynamic shear, with small strain (0.05) and fixed frequency (0.1 Hz), and fractal dimension of Laponite dispersions, after shearing at 50 s^{-1} during 5 min, at a temperature of 22 ± 1 °C. $\phi_v=1.6\%$ and $t_p=53$ days. (a) $C_p=0\%$ tspp, at rest $D_f=1.8$, (b) $C_p=6\%$ tspp, at rest $D_f=1.4$.

the elastic modulus increases quickly and the modulus of viscous dissipation decreases just as quickly. In a further 90 min, the material strengthens to a point where G' is relatively large (1.7×10^3 Pa) and nearly 50 times larger than G''. Subsequently, the evolution is slower. A mechanical and structural analysis of this evolution has been given by Pignon, Magnin, and Piau [24].

In contrast, the mechanical response of the dispersions that contain peptizers shows that they have an essentially viscous behavior after shearing [Fig. 8(b)]. The elastic modulus is inferior to the viscous modulus. After a relatively long time, about 80 min, both moduli cross and the dispersions are still very weak solids. A strong solid is never reached on experimental time scales. The elastic modulus changes progressively over the two characteristic times observed for the dispersion without peptizers. Beyond this characteristic time, the structure is modified over very long times.

In parallel, Fig. 8 shows also the change in the fractal dimension D_f in time, during this recovery of the network. The dispersions that contain no peptizer reform their connected structure very quickly. At short times after shearing, the fractal dimension is slightly lowered by shear flow and at long times it tends to the fractal dimension at rest ($D_f = 1.8$). In contrast, after a preliminary shearing has been stopped, the dispersions that contain peptizers present no fractal organization. D_f increases slowly with time and tends to its value at rest, which is equal to 1.4 at the aging time of our experiments.

This mechanical recovery of the dispersions measures the extent to which a network of mechanical connections has been reestablished. The implication from these results is that dispersions that contain no peptizer are quickly able to reform a fully connected network, because many mechanical links have been preserved. Conversely, dispersions that contain peptizers have a hard time reconstructing a sufficient number of mechanical paths, because the proportion of dissociated links is too high.

D. Behavior in centrifugation

In a centrifugation field, both types of dispersions settled to form concentrated deposits. Their behavior under centrifugation depended on their initial state because they were forced to flow through a syringe in order to fill the centrifugation tubes. Dispersions that contained no peptizer were gels when the centrifugation was started, whereas dispersions that contained peptizers were viscous fluids at the onset of centrifugation.

1. Settling of gelled dispersions

The behavior of dispersions without peptizers was examined in a centrifuge field at an acceleration $A=50\,000g_a$. This behavior is characterized by the change in the deposit volume in time. Figure 9 shows that the gel was progressively compressed, leaving a growing supernatant at the top of the centrifugation tubes. It has been verified that this supernatant was, from the start, practically void of particles.

These results match the well-known behavior of aggregated dispersions in which all particles form a connected network. Consequently, the dispersions without peptizers, initially gelled, contain neither free particles nor small disconnected aggregates. Indeed, if the original dispersions had contained free particles or small aggregates, these would have sedimented only very slowly, and the mass of dry water in the supernatant would not have been equal to zero.

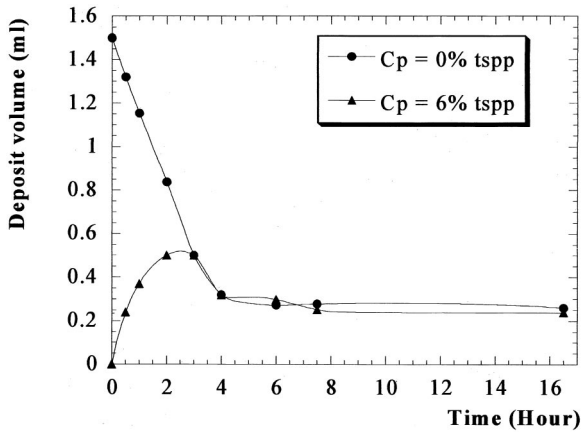

FIG. 9. Deposit volume of laponite dispersions of initial volume fraction 1%, at an acceleration of $50\,000g_a$. $t_p=20$ days.

Hence, it follows that the original gelled dispersions contained a fully connected network of particles. The strength of interparticle interactions that maintain this fully connected network must be consistent with these results.

2. Settling of viscous dispersions

The behavior of dispersions that contain peptizers was also examined in a centrifuge field at an acceleration $A=50\,000g_a$. Figure 9 shows that this behavior was opposite to that of the gelled dispersions. A small deposit was formed at the bottom of the centrifugation tube while most particles initially remained in the supernatant. This deposit grew linearly with time, and then it reached the same volume as that obtained with the other dispersions. Subsequently it was compressed to its equilibrium volume in the centrifugation field. Meanwhile the supernatant became progressively depleted of particles. This is the normal behavior of a fluid dispersion, where individual objects sediment slowly from the supernatant to the deposit.

From this behavior, the average size and density of the objects that sediment could be determined according to the sedimentation laws. In the linear range of the sedimentation curve (Fig. 9), the sedimentation rate may be calculated as

$$V_{\mathrm{sa}}=\frac{\sum_{i=1}^{n-1}\dfrac{V(t_{i+1})-V(t_{i-1})}{S(t_i)(t_{i+1}-t_{i-1})}}{n-1},$$

where n is the number of points in the linear range, $V(t_i)$ and $S(t_i)$ are, respectively, the deposit volume and the section of the tube at a given time. Farrow and Warren [43] have shown that the average diameter D of the objects is

$$D=\sqrt{\frac{18\mu V_{\mathrm{sa}}}{(\rho_a-\rho_l)A}},$$

where A is the acceleration, μ the viscosity of the aqueous phase, ρ_a and ρ_l the density of the objects and the aqueous phase, respectively. ρ_a is determined by

$$\rho_a=\frac{\rho_p+(C_{\mathrm{as}}-1)\rho_l}{C_{\mathrm{as}}},$$

where ρ_p is the density of a particle (Laponite clay in this case) and $C_{\mathrm{as}}=0.62V_{\mathrm{sed}}/V_0\phi_0$ the ratio of the volume of aggregates to the volume of solids. In this relation, V_{sed} is the volume of the deposit, V_0 and ϕ_0 are, respectively, the volume and the volume fraction of dispersions at initial state.

We have checked the validity of these relations by centrifuging dispersions of repelling particles with known diameters. These particles used for this calibration were colloidal spheres of silica manufactured by du Pont de Nemours (Ludox dispersions [44]). They are fairly monodisperse, with core diameters of 22 nm. They are dispersed in an alkaline medium (sodium hydroxide), which reacts with the silica surface to produce a negative charge. Due to this negative charge, the particles repel each other and the dispersions are stable at alkaline pH. The initial volume fraction of the dispersions was 34%.

Using the same relations, we found that the objects that sediment in laponite dispersions with added peptizers have an average diameter $D=31$ nm and an averaged density $\rho_a=1074\ \mathrm{kg\,m^{-3}}$. This density corresponds to the mass fraction of one particle in the volume of its associated sphere of diameter $2R$.

Accordingly, the addition of peptizers weakens the interparticle forces to the point where the interparticle network is fully dissociated by the flow, at the scale of the particle size, and does not recover within the time scale of the centrifugation experiment.

IV. DISCUSSION

The aim of this work was to determine the mechanism of thixotropy in laponite dispersions, i.e., the transformations by which the behavior of the dispersions can change from gel-like to fluid, when they are subjected to sufficient strain, and also change back from fluid to gel-like, when they are left to rest. In order to solve this problem, we can rely on two sets of results: the results of structural experiments, which describe how the particles are organized with respect to each other in the dispersions, and the results of shear and centrifugation experiments, which depend on how they are connected to each other.

A. Structure

According to scattering experiments, the laponite dispersions prepared at moderate ionic strengths are organized according to a hierarchy of spatial scales. We describe this hierarchy starting with the shortest scales (high Q values in the scattering curves) and ending with the longest scales (low Q values).

At very short scales, the relevant distances are distances between each laponite particle and its nearest neighbors. For the concentrated dispersions investigated in this work, these distances are in the range 10–30 nm, and correspond to Q values between 3×10^{-2} and 2×10^{-2} Å^{-1}. At this point, the scattering curves, which have a Q^{-2} decay at higher Q, turn to a plateau that extends from 3×10^{-2} to 2×10^{-3} Å^{-1} (Fig. 4). This plateau indicates that the intensity is depressed with respect to the single particle intensity. By comparing the intensity scattered by the dispersions with the single particle intensity, we have calculated the structure factor of the dispersions [21]. This structure factor shows a depression in the range 1×10^{-2}–2×10^{-3} Å^{-1}, indicating that the concentrations fluctuations are suppressed over this range of distances (i.e., a few interparticle distances). The simplest way to describe that short range order is as a liquidlike order, where each particle sits in a cage formed by its nearest neighbors.

At intermediate scales (Q values ranging from 2×10^{-3} to 2×10^{-4} Å^{-1} in Fig. 4), the intensities are much above the single particle intensities. This excess scattering originates from the alternation of lumps and voids, i.e., at that scale the particles are aggregated into microdomains. In this range the behavior of the intensity is a Q^{-3} power law; this indicates that the microdomains are dense (i.e., they are not mass fractals). Again, the addition of peptizers has no effect at these scales: therefore the microdomains are the same, regardless of whether or not the dispersions contain peptizers.

At larger scales still (Q values below 2×10^{-4} Å^{-1}), the scattered intensities are still higher, but the behavior of the scattering curves is different, and it does depend on peptizer concentration, laponite volume fraction, and sample history. The higher intensity indicates that the microdomains are themselves aggregated, forming a set of superaggregates that extend over macroscopic distances (beyond 30 μm). The power laws are between Q^{-1} and Q^{-2}, indicating that these superaggregates are mass fractals. The variation of the exponents with aging indicates that the aggregation process proceeds over very long time scales. The variation with peptizer concentration indicates that the rate of aggregation is strongly reduced, or inhibited by the addition of peptizers.

The effects of mechanical treatment on these structures have been investigated. We found that the exponents that characterize the structures of the superaggregates are changed by the application of shear (Fig. 8). In dispersions that were examined shortly after strong mechanical treatment, the intensity is flat at low Q values, indicating that the microdomains are disconnected from each other. Then, during rest time, the exponents rise again, indicating that the microdomains reassociate and form superaggregates, which are tenuous at first, and later become branched and bushy.

B. Connections

According to centrifugation experiments, gelled dispersions contain a fully connected network of particles (there

are very few free particles). According to scattering experiments, this network is made by the connection of microdomains into superaggregates, and of superaggregates to each other.

These dispersions can be forced to flow by applying sufficient strain; therefore the network can be disrupted by shear. This fluidlike behavior can be maintained if continuous shear is applied (long time limit in Fig. 7). However, in dispersions that contain no peptizers, the network is formed again (in less than 1 s) as soon as the dispersions are brought to rest, and consequently the fluid state is lost. Indeed, the mechanical response of these dispersions shows a dominant elastic modulus right after the end of shear [Fig. 8(a)].

In dispersions that contain peptizers, the fluid state lasts for longer times, and a fluidlike behavior was observed through measurements of the mechanical response [$G' < G''$ in Fig. 8(b)]. This was also confirmed by centrifugation experiments, where slow sedimentation of individual particles was observed over similar time scales. However, when the dispersions were kept at rest for extended lengths of time (over 5×10^3 s), it was found that the continuous aggregation processes generated a new network of superaggregates [rising exponents of the scattering curves, presented in Fig. 8(b)], and the mechanical response became predominantly elastic again ($G' > G''$).

Accordingly, the thixotropy of laponite dispersions originates from the forced disruption of the network of connected particles, and the spontaneous reconnection of this network during rest. The main effect of peptizers is to slow down this reformation process.

C. Interactions

These results raise some questions concerning the nature of interactions that make it possible to disrupt the network so easily, and to have it reform slowly, but completely. In colloidal dispersions, the interactions between particles may be either repulsive or attractive. In laponite dispersions made at moderate ionic strength, there are evidences for both repulsive and attractive interactions. The repulsive interactions are demonstrated by the depression of the scattering curves in the range of Q values (2×10^{-3}–2×10^{-4} Å^{-1} in Fig. 4) corresponding to distances between neighboring particles. The attractive interactions are demonstrated by the rise in the scattering curves at lower Q values. We have analyzed this excess scattering as being produced by dense microdomains, which are themselves connected into superaggregates (Q^{-3} power law in the range 2×10^{-3}–2×10^{-4} Å^{-1}, followed by another power law at lower Q values). The centrifugation experiments also confirm that the dispersions are made of a fully connected network of superaggregates, separated by voids that contain practically no free particles.

The repulsive interactions, evidenced by the plateau in the scattering curves, are always presenting dispersions of high volume fractions, regardless of peptizer concentration and aging. They must originate form excluded volume effects, as in other colloidal dispersions. The attractive interactions, evidenced by the excess scattering at low Q, are disrupted by the effects of peptizers and mechanical treatment (the excess scattering is reduced, and the exponent is changed, as shown in Fig. 8). Peptizers are ions that bind specifically to the edges of the laponite platelets. Therefore, the peptizers may inhibit some edge-to-face attractions of neighboring particles. Accordingly, the formation of the network results from edge-to-face attractions, which are weakened or suppressed by the adsorption of peptizers on the edges.

V. CONCLUSION

In laponite dispersions made at moderate ionic strengths (above 10^{-3} mol l^{-1}) and high pH, the particles are aggregated into dense microdomains, which are themselves connected into superaggregates. These superaggregates form a network that controls the mechanical properties of the dispersions.

The interactions that cause these aggregation processes are electrostatic attractions between particles in edge-to-face configurations. They are weakened by the addition of peptizers that bind to the positively charged surface sites on the edges of the platelets and weaken their association with the negatively charged sites on the faces of the platelets. In the absence of peptizers, the network that results from edge-face interactions can be disrupted by shear, but it reforms immediately when shear is interrupted. In the presence of peptizers, the network forms slowly, and the fluid state can be retained for extended lengths of time after the end of mechanical treatment. These liquid-gel transitions correspond to the network crossing the percolation threshold in either direction.

Thus, the thixotropic behavior of laponite dispersions (i.e., a mechanical response that depends on history) originates from the changes in a network of superaggregates that extends throughout the dispersion; this behavior can be controlled by manipulating the balance of repulsive and attractive interactions of the particles.

[1] Laporte Industries Ltd., Laponite Technical Bulletin, **L104/90/A**, 1 (1990).
[2] R. G. Avery and J. D. F. Ramsay, J. Colloid Interface Sci. **109**, 448 (1986).
[3] B. S. Neumann and K. G. Sansom, Isr. J. Chem. **8**, 315 (1970).
[4] B. S. Neumann and K. G. Sansom, Clay Miner. **8**, 389 (1970).
[5] B. S. Neumann and K. G. Sansom, Clay Miner. **9**, 231 (1971).
[6] J. Fripiat, J. Cases, M. Francois, and M. Letellier, J. Colloid Interface Sci. **89**, 378 (1982).
[7] J. D. F. Ramsay, R. G. Avery, and L. Benest, Faraday Discuss. Chem. Soc. **76**, 53 (1983).
[8] J. D. F. Ramsay, S. W. Swanton, and J. Bunce, J. Chem. Soc., Faraday Trans. **86**, 3919 (1990).
[9] L. Rosta and H. R. Von Gunten, J. Colloid Interface Sci. **134**, 397 (1990).
[10] D. W. Thomson and J. T. Butterworth, J. Colloid Interface Sci.

151, 236 (1992).
[11] J. Plaizier-Vercammen, Pharmazie **47**, 856 (1992).
[12] J. D. Sherwood, J. Non-Newtonian Fluid Mech. **43**, 195 (1992).
[13] J. D. F. Ramsay and P. Lindner, J. Chem. Soc., Faraday Trans. **89**, 4207 (1993).
[14] M. Morvan, D. Espinat, J. Lambard, and Th. Zemb, Colloids Surf., A **82**, 193 (1994).
[15] A. Mourchid, A. Delville, J. Lambard, E. Lécolier, and P. Levitz, Langmuir **11**, 1942 (1995).
[16] A. Mourchid, A. Delville, and P. Levitz, Faraday Discuss. **101**, 275 (1995).
[17] J. C. P. Gabriel, C. Sanchez, and P. Davidson, J. Phys. Chem. **100**, 11 139 (1996).
[18] F. Pignon, A. Magnin, and J. M. Piau, J. Rheol. **40**, 573 (1996).
[19] F. Pignon, J. M. Piau, and A. Magnin, Phys. Rev. Lett. **76**, 4857 (1996).
[20] M. Kroon, G. H. Wegdam, and R. Sprik, Phys. Rev. E **54**, 6541 (1996).
[21] F. Pignon, A. Magnin, J. M. Piau, B. Cabane, P. Lindner, and O. Diat, Phys. Rev. E **56**, 3281 (1997).
[22] F. Pignon, A. Magnin, and J. M. Piau, Phys. Rev. Lett. **79**, 4689 (1997).
[23] M. Kroon, W. L. Vos, and G. H. Wegdam, Phys. Rev. E **57**, 1962 (1998).
[24] F. Pignon, A. Magnin, and J. M. Piau, J. Rheol. **42**, 1349 (1998).
[25] A. Mourchid, E. Lécolier, H. Van Damme, and P. Levitz, Langmuir **14**, 4718 (1998).
[26] A. Mourchid and P. Levitz, Phys. Rev. E **57**, R4887 (1998).
[27] D. Bonn, H. Tanaka, G. Wegdam, H. Kellay, and J. Meunier, Europhys. Lett. **45**, 52 (1999).
[28] P. Levitz, E. Lécolier, A. Mourchid, A. Delville, and S. Lyonnard, Europhys. Lett. **49**, 672 (2000).
[29] D. Bonn, H. Kellay, H. Tanaka, G. Wegdam, and J. Meunier, Langmuir **15**, 7534 (1999).
[30] J. M. Saunders, J. W. Goodwin, R. M. Richardson, and B. Vincent, J. Phys. Chem. B **103**, 9211 (1999).
[31] E. Dickinson, J. Colloid Interface Sci. **225**, 2 (2000).
[32] P. Dietler, C. Aubert, D. S. Cannel, and P. Wiltzius, Phys. Rev. Lett. **57**, 3117 (1986).
[33] J. A. Yanez, E. Laarz, and L. Bergström, J. Colloid Interface Sci. **209**, 162 (1999).
[34] J. Persello, A. Magnin, J. Chang, J. M. Piau, and B. Cabane, J. Rheol. **38**, 1845 (1994).
[35] M. Gradzielski, M. Bergmeier, M. Müller, and H. Hoffmann, J. Phys. Chem. B **101**, 1719 (1997).
[36] S. Jogun and C. F. Zukoski, J. Rheol. **40**, 1211 (1996).
[37] N. C. Lockhart, J. Colloid Interface Sci. **74**, 509 (1980).
[38] P. Lindner and R. C. Oberthür, Rev. Phys. Appl. **19**, 759 (1984).
[39] J. M. Piau, in *Crucial Elements of Yield Stress Fluid Rheology*, edited by M. J. Adams, R. A. Mashelkar, J. R. A. Pearson, and A. R. Rennie (Imperial College Press, London, 1997).
[40] J. M. Piau, M. Dorget, J. F. Palierne, and A. Pouchelon, J. Rheol. **43**, 305 (1999).
[41] M. Dorget, Ph.D thesis, the Institut National Polytechnique de Grenoble France, 1995.
[42] A. Magnin and J. M. Piau, J. Non-Newtonian Fluid Mech. **36**, 85 (1990).
[43] J. Farrow and L. Warren, Coagulation and flocculation **47**, 391 (1993).
[44] K. Wong, P. Lixon, F. Lafuma, P. Lindner, O. Aguerre Charriol, and B. Cabane, J. Colloid Interface Sci. **153**, 55 (1992).